Dimensional analysis of a planetary mixer for homogenizing of free flowing powders: Mixing time and power consumption

C. Andre, Jean-François Demeyre, Cendrine Gatumel, Henri Berthiaux, G. Delaplace

Dimensional analysis of a planetary mixer for homogenizing of free flowing powders: Mixing time and power consumption

C. André [a,b,*], J.F. Demeyre [c], C. Gatumel [c], H. Berthiaux [c], G. Delaplace [a]

[a] INRA, U.R. 638 Processus aux Interfaces et Hygiène des Matériaux, F-59651 Villeneuve d'Ascq, France
[b] UC Lille, Hautes Etudes Ingénieurs (H.E.I.), Laboratoire de Génie des Procédés, 13 Rue de Toul, 59046 Lille, France
[c] Université de Toulouse, Centre RAPSODEE, Ecole des Mines d'Albi-Carmaux, Campus Jarlard, 81013 Albi Cedex 09, France

- ▶ An innovative planetary mixer was used for homogenizing free flowing powders.
- ▶ Mixing times were determined using a method based on image processing.
- ▶ Dimensional analysis was validated by experimental results.
- ▶ Generalized power and mixing numbers were defined.
- ▶ Θ_M represents the path to achieve an imposed degree of homogeneity.

Keywords:
Mixing time
Power consumption
Planetary mixer
Free flowing powder
Dimensional analysis

A B S T R A C T

Powder mixing is crucial to the processing stages in many industries. However, there is still a paucity of information about the effects of process parameters on mixing efficiency. This paper investigates the homogenization of free flowing granular materials with a planetary mixer, TRIAXE®, examining the effect of the ratio of impeller rotational speeds (N_R/N_G) on the mixing process.

First, a dimensional analysis carried out with mixing time and power consumption as target variables, established that both a Froude number and N_R/N_G controlled the process for the given free flowing powder mixture and planetary mixer.

A further theoretical approach also suggested that these two dimensionless ratios which control hydrodynamics can be reduced to a modified Froude number providing that the maximum linear velocity achieved (u_{ch}) by the planetary mixer is introduced, replacing the dual impeller rotational speeds (N_R and N_G).

Mixing time and power experiments validated the above hypothesis. Homogeneity tests performed in a granular media showed that the length of path achieved by the impeller governs the obtained mixing level.

Finally, this work reflected that (i) dimensional analysis was also well suited to model powder homogenization with a planetary mixer. (ii) A concise set of dimensionless numbers governing mixing phenomena can be deduced through the introduction of the maximum linear velocity as obtained in previous studies on gas/liquid and miscible liquids mixing processes.

1. Introduction

Powder mixing is an important unit operation in a wide variety of industries involved in solids processing. The end-use properties of products of the pharmaceutical, food, plastics and fine chemicals industries, often depend on process history which includes thermal and mechanical actions of dry mixers and/or contact machines (e.g. for encapsulation, agglomeration, etc.). These properties are usually determined through a formulation procedure involving costly evaluations of biological activities to determine the composition, dosage and form of a drug. Although constant efforts are devoted to this aspect, little is known about the manufacturing process itself which makes the study of mixing and mixtures a key subject for both academic and industrial product and process engineers [1–3].

Once a scale of scrutiny of a mixture is set, its homogeneity is usually defined on a statistical basis, considering samples of like size. In industrial practice, when n samples are considered, the

* Corresponding author at: UC Lille, Hautes Etudes Ingénieurs (H.E.I.), Laboratoire de Génie des Procédés, 13 Rue de Toul, 59046 Lille, France.
E-mail address: christophe.andre@hei.fr (C. André).

Nomenclature

c_b	bottom clearance, m
d	characteristic length, m
d_{p1}	diameter of powder 1, m
d_{p2}	diameter of powder 2, m
d_s	diameter of horizontal part of planetary mixer, m
D	diameter of turbine part, m
Fr	Froude number
Fr_G	Froude number based on gyrational speed of agitator
Fr_M	generalized Froude number based on tip speed
H	agitator height, m
H_L	liquid height, m
N	speed of agitator, s^{-1}
N_G	gyrational speed of agitator, s^{-1}
N_R	rotational speed of agitator, s^{-1}
Np	power number
N_{pG}	power number based on gyrational speed of agitator
Np_M	generalized power number based on tip speed
P	power, W
t	time, s
t_m	mixing time, s
$t_{m99\%}$	mixing time for X_M = 0.99, s
T	vessel diameter, m
u_{ch}	maximum tip speed of agitator, m s^{-1}
$u_{impeller\ tip}$	impeller tip speed, m s^{-1}
x	massic composition of the powder
X_M	mixing index

Greek letters

μ	viscosity of viscous medium, Pa s
ρ	density of viscous medium, kg m^{-3}
ρ_1	density of powder 1, kg m^{-3}
ρ_2	density of powder 2, kg m^{-3}
Θ	mixing time number
Θ_G	modified mixing time number based on gyrational speed of agitator
Θ_M	modified mixing time number based on the characteristic speed u_{ch}
σ^2	experimental value of the variance
σ_0^2	initial value of the variance
σ_∞^2	minimum value of the variance

homogeneity of a mixture is judged by comparing the coefficient of variation (CV) of the distribution of the sample composition of a key ingredient to a standard value. In the pharmaceutical industry, a mixture exhibiting a coefficient of variation greater than 6% is rejected as non-conform [4]. The variance σ^2 of the mixture can also be used. For batch operations, the dynamics of the mixing process are monitored by examining the changes of variance with time. Such a curve usually features a quick decrease in variance due to the efficiency of convection mechanisms in reducing the intensity of segregation at a macro scale, followed by a much slower decrease due to micro scale particle diffusion. This latter plateau region sometimes exhibits oscillations which are classically attributed to a competition in particle segregation. Mixing kinetics determine mixing time, the time corresponding to the smallest value of variance [5–8].

Different mixer geometries and agitation devices exist usually based on empirical methods [9]. The use of chemical engineering tools, such as correlations between dimensionless numbers, ought to be considered to improve knowledge on the mixing powder media [10]. However, the traditional method of dimensional analysis applied for liquids including a Reynolds number cannot be derived since no apparent viscosity can be introduced. As such, empirical correlations involving Froude number have often been used for many systems: generalities and correlations [11,12]. One may refer to the correlations of Sato et al. for a horizontal drum mixer [13] or a ribbon mixer [14], the relations of Entrop for a screw mixer [15]. Planetary mixers are often used to optimize mixing processes. Pioneer and more intensive works on non-conventional mixers have been conducted by Tanguy and co-workers. However, if we focus only on planetary mixers defined as combining dual revolution motion around two axes, the literature is still scarce [16–23]. Most of these works concern mixing of miscible fluids. Few of them deal with foaming fluids [24] or granular media [25].

For the investigated planetary mixer (the Triaxe system), Delaplace et al. [22,23] proposed a definition of power and mixing numbers when mixing viscous liquids. Originally built for operating with viscous fluids [21], this mixer has also shown its capability to achieve good mixtures of granular products [25]. However, currently, there is a lack of knowledge concerning dimensionless ratios controlling the mixing of granular materials with such a Triaxe system. The objectives of this work are twofold: (i) to perform dimensional analysis governing mixing time and power consumption in a planetary mixer for the case of granular materials, (ii) to validate this approach by experimental results obtained with a pilot-scale planetary mixer.

2. Theory

2.1. Dimensional analysis for conventional mixing in solid phase

An agitated vessel without baffles equipped with an impeller mounted vertically and centrally is schematically shown in Fig. 1.

For such a mixing system subjected to a gravity field, with a given stirrer type and under given installation conditions (vessel diameter, agitator height, bottom clearance and solid height, see Fig. 1), mixing time t_m depends on agitator diameter, material parameters of the medium (densities (ρ_1, ρ_2), particle size (d_{p1}, d_{p2}) and solid/solid fraction (x)) and speed of the agitator:

$$F_1(t_m, d, T, H, C_b, \rho_1, \rho_2, d_{p1}, d_{p2}, x, N, g) = 0 \quad (1)$$

Introducing $\Delta\rho = \rho_2 - \rho_1$, this list of relevant parameters can be rewritten as

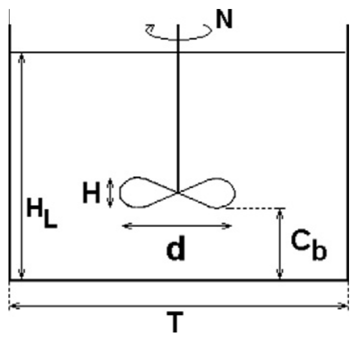

Fig. 1. Classical geometric parameters and notations used for mixing vessel equipped with an impeller vertically and centrally mounted in a tank.

$$F_2(t_m, d, T, H, C_b, \rho_1, \Delta\rho, d_{p1}, d_{p2}, x, N, g) = 0 \quad (2)$$

Taking (N, ρ_1, d) as reference parameters to form the π-terms, dimensional analysis considerably reduces the dependent variables as follows [26]:

$$F_3\left(\Theta, T/d, H/d, C_b/d, \frac{\Delta\rho}{\rho_1}, \frac{d_{p1}}{d}, \frac{d_{p2}}{d}, x, Fr\right) = 0 \quad (3)$$

where $\Theta = N \cdot t_m$ is the so-called mixing time number or mixing number and $Fr = N^2 \cdot d/g$ is the Froude number. For a given mixing system (tank + agitator) and fixed position of the agitator in the vessel, geometrical ratios are constant. When the characteristics of the two powders (particle sizes, compositions, densities) are fixed, Eq. (3) is further reduced to a single dependence between Θ and Fr.

$$F_4(\Theta, Fr) = 0 \quad (4)$$

A similar analysis concerning the consumption of power, P as target variable, can be made and led to following equation:

$$F_5(N_p, Fr) = 0 \quad (5)$$

where $N_p = \frac{P}{\rho_1 \cdot N^3 \cdot d^5}$ is the power number.

To sum up, both Θ and N_p are target ratios which are dependent only on the Froude number for a fixed mixer and given characteristics of the powder mixture. F_i (for i ranging from 3 to 5) are process relationships which linked target ratios to other π-terms governing transport phenomena.

2.2. Dimensional analysis of a planetary mixer in solid phase

Similar to the above case, the relevant dimensional parameters influencing the mixing time with the TRIAXE® system can be written as:

$$F_6(t_m, D, d_s, T, C_b, H_L, \rho_1, \Delta\rho, d_{p1}, d_{p2}, x, N_R, N_G, g) = 0 \quad (6)$$

In Eq. (6), N_R and N_G are rotational and gyrational speeds respectively; D, T, C_b and d_s are the geometric parameters reported in Fig. 2. H_L refers to the powder height.

For fixed installation conditions, taking (N_G, ρ_1, d_s) as reference parameters to form the π-terms, this 14-parametric dimensional space leads to a power characteristic consisting of three pi-numbers:

$$F_7\left(\Theta_G, Fr_G, \frac{N_R}{N_G}\right) = 0 \quad (7)$$

where $\Theta_G = N_G \cdot t_m$ and $Fr_G = N_G^2 \cdot d_s/g$.

A same analyse concerning the power P can be made.

$$F_8(P, D, d_s, T, C_b, H_L, \rho_1, \Delta\rho, d_{p1}, d_{p2}, x, N_R, N_G, g) = 0 \quad (8)$$

Taking (N_G, ρ_1, d_s) as reference parameters to form the π-terms, power characteristic reduced to interdependence of the following 3-parametric pi-set:

$$F_9\left(N_{pG}, Fr_G, \frac{N_R}{N_G}\right) = 0 \quad (9)$$

where $N_{pG} = \frac{P}{\rho_1 \cdot N_G^3 \cdot d_S^5}$.

Note that in Eqs. (7)–(9), the variables (N_G, ρ_1, d_s) have been taken as reference parameters to form the π-terms. This choice allows, in the absence of rotational motion of the planetary mixer (i.e. $N_R = 0$), sets of π-numbers describing mixing time and power consumption to become similar to those commonly used with a classical mixing system (Fig. 3). This result was expected since, when $N_R = 0$, a planetary mixer runs like a traditional mixer.

It is of obvious importance to reduce the number of variables in the reference list to minimize the set of π numbers defining the transport phenomena. Consequently, it is of major importance to consider introducing into the reference list intermediate variables able to concisely take into account and replace the effect of other groups of variables. A characteristic velocity u_{ch}, characterizing the intensity of the flow due to the dual motion of the impeller, is such an intermediate quantity. This characteristic velocity can replace all the corresponding dimensional variables as shown below:

$$F_{10}(t_m, D, d_s, T, C_b, H_L, \rho_1, \Delta\rho, g, d_{p1}, d_{p2}, x, u_{ch}) = 0 \quad (10)$$

Taking (u_{ch}, ρ_1, d_s) as reference parameters to form the π-terms allows us to reduce interdependence of the mixing characteristic to the following 2-parametric π set for fixed granular media and planetary mixer:

$$F_{11}(\Theta_M, Fr_M) = 0 \quad (11)$$

with $\Theta_M = t_m \cdot u_{ch}/d_s$ and $Fr_M = u_{ch}^2/(g \cdot d_s)$.

A same analysis concerning the power P led to Eq. (12)

$$F_{11}(N_{pM}, Fr_M) = 0 \quad (12)$$

where $N_{pM} = \frac{P}{\rho_1 \cdot u_{ch}^3 \cdot d_S^2}$.

It is not trivial to define which characteristic velocity should be taken as reference for a planetary mixer but its definition becomes logical if we keep in mind that the characteristic velocity used for a classical mixing system is $N_G \cdot d_s$.

For a classical mixing system, the impeller tip speed (m/s) is defined as $u_{\text{impeller tip}} = 2 \cdot \pi \cdot N_G \cdot d_s/2$. This impeller tip speed represents the average but also the maximum velocity (m/s) which could be achieved by an element of fluid in the tank. So, for a classical mixing system, the characteristic velocity $N_G \cdot d_s$ is nothing other than the impeller tip speed divided by π. Contrary to classical

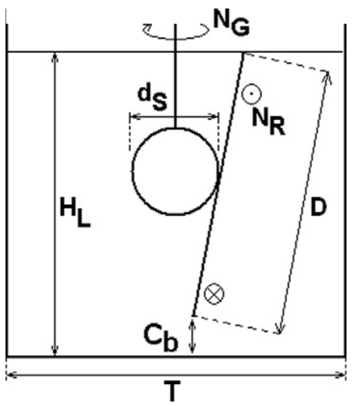

Fig. 2. Sketch and symbols used for the TRIAXE® system investigated.

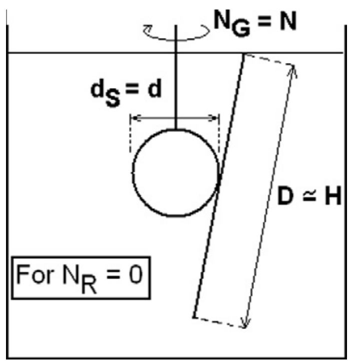

Fig. 3. Analogies between the geometric parameters of the classical mixing system and the TRIAXE® planetary mixer when rotational speed is set to zero.

mixing systems, the instantaneous impeller tip speed $u_{\text{impeller tip}}(t)$ in an inert reference frame is not a constant value with time t. Nevertheless, it is possible to deduce from analytical expression of the impeller tip speed its maximum value which represents also the highest velocity that an element of fluid can reach: $\max(u_{\text{impeller tip}})$.

The only way to obtain a characteristic velocity having a similar physical meaning, as obtained with a classical mixing system, is to take the maximum velocity which could be encountered by the agitated media $\max(u_{\text{impeller tip}})$ and then to divide it by π.

$$u_{ch} = \max\left(u_{\text{impeller tip}}(t)\right)/\pi \tag{13}$$

This expression of $u_{\text{impeller tip}}(t)$ and its maximum $\max(u_{\text{impeller tip}}(t))$ have been established elsewhere [22]. The maximum value depends on the value of the ratio N_R/N_G. Its final expression is given by the following equations:

$$\text{when } N_R \cdot d_s/N_G \cdot D < 1 : u_{ch} = (N_R \cdot D + N_G \cdot d_s) \tag{14}$$

$$\text{when } N_R \cdot ds/N_G \cdot D < 1 : u_{ch} = \sqrt{\left(N_R^2 + N_G^2\right) \cdot \left(d_s^2 + D^2\right)} \tag{15}$$

To sum up, dimensional analysis of the TRIAXE® mixer for homogenizing granular materials in a fixed installation, led to either a relationship between three (Eqs. (7) and (9)) or two π numbers (Eqs. (11) and (12)). The latter was possible when the characteristic speed, proportional to the maximum impeller tip speed, was introduced into the parametric dimensional space. In addition, it has been shown that the π numbers reduced to well-known Froude, mixing time and power numbers when the rotational speed is zero, which was expected since in this case a planetary mixer runs like a classical mixer.

3. Materials and methods

3.1. Mixing equipment

The mixer used in this work was a TRIAXE® system (TriaProcess, France) which combines two motions: gyration and rotation (cf. Fig. 4).

Gyration is the revolution of the agitator around a vertical axis while rotation is a revolution of the agitator around a nearly horizontal axis. This dual motion allows the agitator to sweep the entire volume of the vessel. The mixing element of the TRIAXE® system is a pitched four blade turbine and the axes of the two revolutionary motions are nearly perpendicular driven by two variable speed motors. The mixing vessel is a stainless steel sphere, the blades of the agitator pass very close to the vessel wall in less than a millimeter. For all the experiments, the mass of powder was maintained to 33.35 kg. The overall power P was determined using torque and impeller speeds measurements. P refers to the net power. Net power is deduced from loaded power minus unloaded power (power monitored at the fixed impeller rotational speeds when no powder is present in the tank).

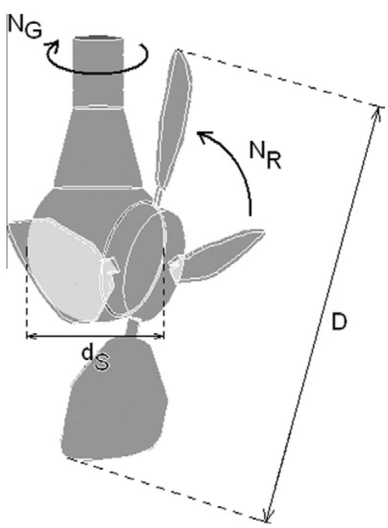

Fig. 4. Diagram of the TRIAXE® system investigated (d_s = 0.14 m and D = 0.38 m).

3.2. Particulate system involved

The solids used are free flowing powders (couscous and semolina). The true densities of the semolina and the couscous were measured with a Helium pycnometer (Accumulator Pyc 1330, Micromeritics). The packed densities were measured by a volumenometer. A powder mass is introduced into a graduated test-tube of 250 cm^3 and the bulk volume is recorded after a certain number of standard taps (500 taps). We can note that the densities of the powders are similar (see Table 1). From these values, the Carr index (IC) to evaluate the flowability [27] as well as the Hausner ratio (HR) to evaluate the compressibility of the powder [28], were determined. It is widely admitted that free flowing powders have low IC (<18%) and low HR (<1.25). In contrast, cohesive, high compressive powders have high IC (>20%) and high HR (>1.4).

The particle size distribution of the couscous was obtained by sieving using a vibrating sieve Retsch® under defined conditions (mean amplitude and 3 min vibration). Sieving was performed using a standard set of sieves. The particle size distributions of semolina and mixtures of semolina and couscous were obtained by laser diffraction using a Mastersizer® particle size analyzer operating under its dry mode see Table 2: d_x is the particle diameter, for which x% of the particles distribution has a diameter smaller than this value.

3.3. Mixing operation and determination of mixing time

Only binary mixtures were considered. Couscous was stained with a mixture of iodine, betadine and ethanol, giving it a black color in order to be contrasted with semolina during image analysis. Semolina is light colored and smaller in size. These components were chosen because they could easily be re-used after sieving, and also to define experimental conditions favoring segregation which makes the homogenization process difficult. Optical methods were developed in order to determine mixing time in granular mixing processes [29–31]. In this study, a method based on image processing using a camera Lord DVL 5000 T was developed under Labview in order to determine the homogeneity level of the mixture at any given time of the batch process [24]. Since the granular medium consists of only two powders, a threshold was applied to each image in order to distinguish couscous from semolina. The ratio of black pixels to white led to the couscous proportion. A calibration curve was established to convert pixel proportion into mass composition (Fig. 5).

Table 1
Densities and properties of the powders.

Density (kg l^{-1})	Semolina	Couscous	Couscous/semolina
True[a]	1.45	1.43	1.45
Aerated[b]	0.76	0.72	0.71
Packed (500 taps)[b]	0.82	0.76	0.96
Carr index	7.3%	5.3%	12.03%
Hausner ratio	1.08	1.06	1.14

[a] Established with the Helium pycnometer.
[b] Established with a volumenometer.

Table 2
Characteristic particle diameters of semolina and couscous.

Diameter (μm)	Semolina[a]	Couscous[b]	Couscous/semolina[a]
d_{10}	200	1100	266
d_{50}	340	1400	412
d_{90}	840	1800	1304
Span = $(d_{90} - d_{10})/d_{50}$	1.88	0.5	2.52

[a] Established with the laser particle-measurement instrument.
[b] Established by sifting.

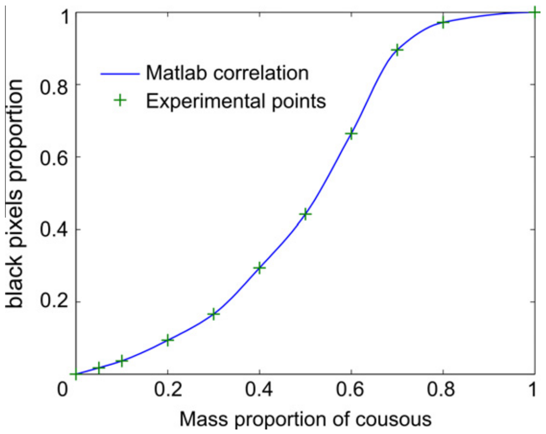

Fig. 5. Calibration curve.

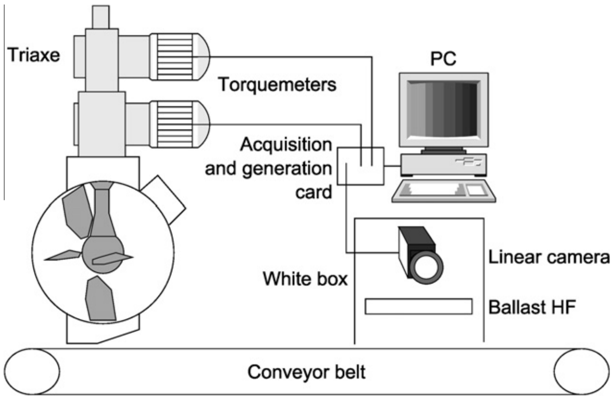

Fig. 6. Experimental set-up.

The experimental set-up is shown in Fig. 6.

Each experiment was performed according to the following procedure: (i) Fill the vessel with a known mass of each component: 7 kg of couscous and 26.35 kg of semolina. (ii) Introduce these components manually, starting with the introduction of couscous. (iii) Start the agitation at the speeds directly selected. (iv) Stop the mixer at a chosen time. (v) Empty the mixer to a conveyor passing under the image processing system. The composition of the mixture was chosen in order to optimize the precision of the image treatment according to the calibration curve behavior. The whole medium is thus analyzed, drastically reducing sampling errors. This protocol is summarized in Fig. 7.

For any given experimental condition, the variance σ^2 was obtained and plotted as a function of time. A mixing index X_M was defined [32–34].

$$X_M = \frac{\sigma_0^2 - \sigma^2}{\sigma_0^2 - \sigma_\infty^2} \tag{16}$$

σ_0^2 corresponds to the initial state (total segregation), σ_0^2 is given by Eq. (17)

$$\sigma_0^2 = x \cdot (1 - x) \tag{17}$$

In Eq. (17), x represents the mass fraction of couscous in the mixture, σ_∞^2 is the minimum value of σ^2 in the kinetic curve. Mixing time $t_{m99\%}$ was determined when X_M achieved the value of 0.99, leading to a limit value of σ^2, of 0.00207 (see Fig. 8).

Experiments were carried out for various ratios of gyration and rotation speeds. The ratios are represented as shown in the first column of Table 3. For example, G100R200 refers to a mixing process performed with a gyration and a rotation speed of 10% and 20% of full speed range.

4. Results and discussion

Mixing time and power measurements obtained for the TRI-AXE® system are shown in Table 3. The obtained mixing time was in between 52 and 367 s for different speed ratios. Increase in the speed of any one motion obviously decreased mixing time.

When mixing time is presented in terms of dimensionless numbers (Θ_G versus Fr_G) as defined in Eq. (9), Θ_G appears to be a constant for the range of Fr_G investigated varying only significantly with N_R/N_G. The range of Θ_G is between 1 and 22. (cf. Fig. 9).

Θ_G represents the number of revolutions made around the vertical shaft required to obtain the desired homogeneity level. Results show that this number of revolutions is highly dependent on the intensity of N_R/N_G, which is the number of rotations around the horizontal axis made by the agitator during one gyrational revolution. High values of N_R/N_G mean that the volume of granular media contained in the vicinity of the blade is swept out by the rotational motion at high frequency. Consequently, good overall dispersion of the powders is obtained in a single revolution of the blade around the vertical shaft in the vessel. In Fig. 9, it can be observed that the gyration number Θ_G to achieve homogeneity is equal to 1, until N_R/N_G reaches a value of 26. It can be observed that a higher value of N_R/N_G (69 in Fig. 9) is not necessary and

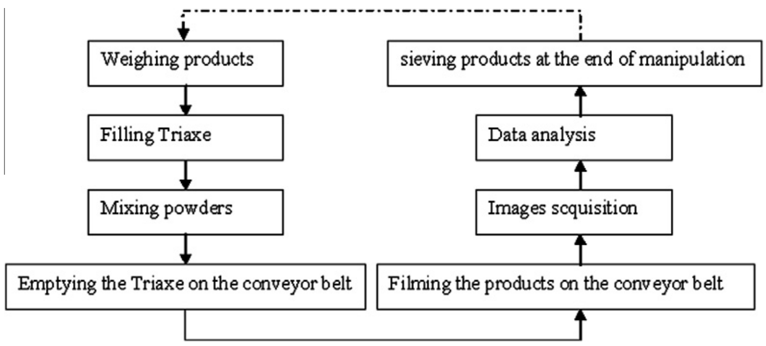

Fig. 7. Diagram of the experimental protocol.

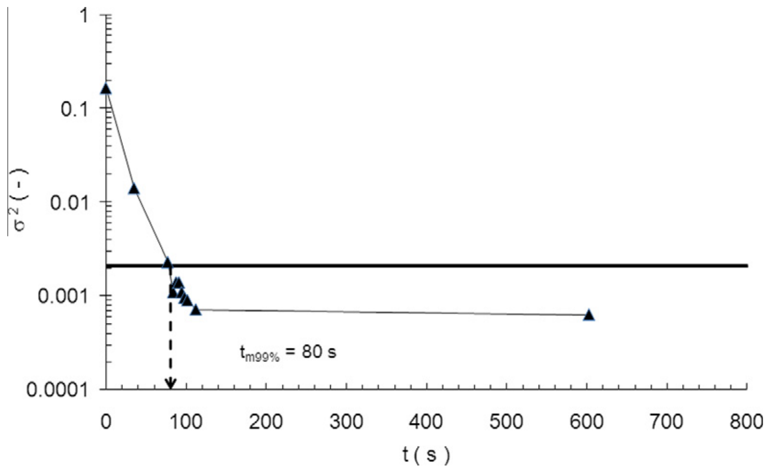

Fig. 8. Determination of mixing time t_m.

Table 3
Experimental conditions and experimental results.

Run names	N_G (s^{-1})	N_R (s^{-1})	t_m (s)	P (W)
G200R50	0.069	0.114	309	31
G50R100	0.017	0.157	367	32
G300R75	0.104	0.171	125	46
G100R200	0.035	0.314	153	67
G800R75	0.276	0.273	80	83
G600R150	0.207	0.343	97	95
G50R300	0.017	0.451	81	102
G800R200	0.276	0.457	70	117
G200R400	0.069	0.629	132	143
G200R600	0.069	0.923	52	207
G400R600	0.138	0.964	62	224
G800R600	0.276	1.045	54	249
G50R800	0.017	1.187	67	270
G400R800	0.138	1.258	56	294

cannot improve mixing. Conversely, it is also shown in Fig. 9 that when the speed ratio is close to 1, the number of revolutions around the vertical shaft to achieve homogeneity becomes high, and equal to 22. In this case, the contribution of rotational motion in the homogeneity process is weak; only gyrational motion contributes to dispersion.

In contrast, it is shown in Fig. 10 that the use of modified Froude and mixing time numbers involving the characteristic speed u_{ch}, as suggested in Eq. (11), considerably reduces the influence of N_R/N_G on Θ_M values. Θ_M values were found between 89 and 240. The ratio between the minimum and maximum values is reduced to 2.7 (in Fig. 10) compared to 22 (in Fig. 9). This result proves the feasibility to obtain a unique mixing curve when u_{ch}, characterizing the overall flow, is introduced.

The fact that Θ_M is nearly constant agrees with the results obtained with classical or planetary mixing systems when mixing highly viscous fluids under laminar regime [23]. Θ_M can be considered as the length of path achieved by the impeller to obtained the desired level of homogeneity. This constant value proved that the degree of homogeneity in the planetary mixer, whatever the speed ratio, is controlled by this length of path made by the impeller.

Finally, as the average value of Θ_M was found to be 150, it can be deduced that mixing times of the planetary mixer are:

$$\text{when } N_R \cdot d_s/N_G \cdot D < 1 : t_m = \frac{150 \cdot d_s}{\sqrt{(N_R^2 + N_G^2) \cdot (d_s^2 + D^2)}} \quad (18)$$

$$\text{when } N_R \cdot d_s/N_G \cdot D > 1 : t_m = \frac{150 \cdot d_s}{(N_R \cdot D + N_G \cdot d_s)} \quad (19)$$

Of course, it cannot be ignored that the emptying operation could disturb the real homogeneity situation existing in the mixer. Nevertheless, the fact that mixing time data (measured after emptying) are still strongly dependent on the impeller rotational speed ratio (N_R/N_G) shows that the emptying is not in capacity to

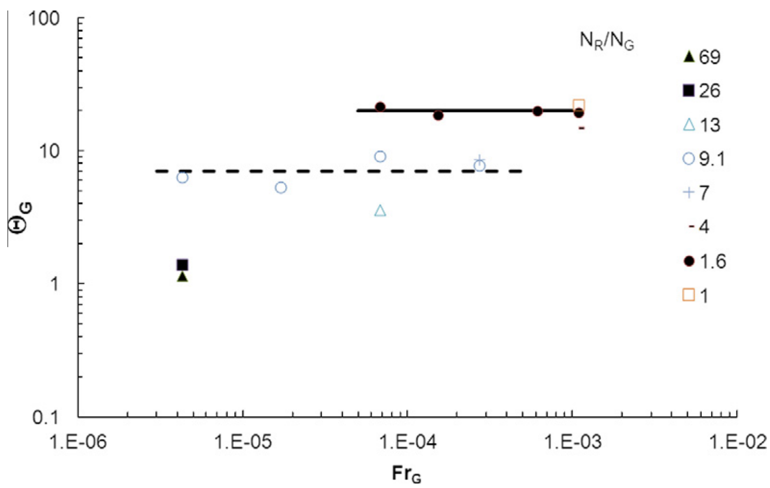

Fig. 9. Evolution of Θ_G against Fr_G.

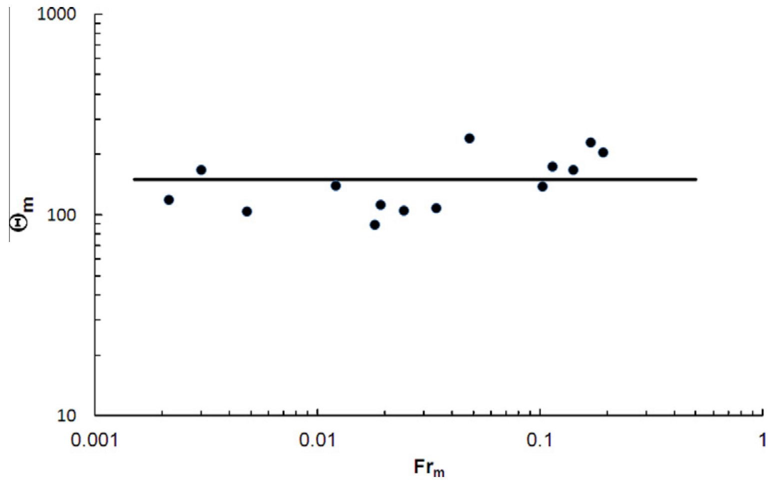

Fig. 10. Evolution of Θ_M against Fr_M.

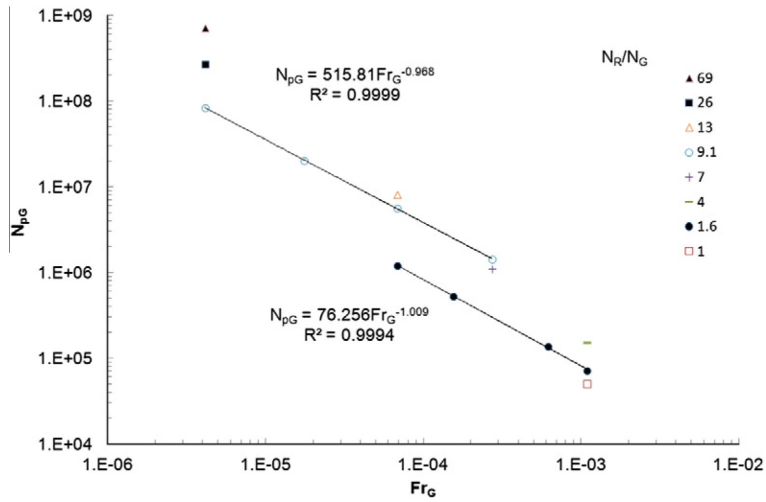

Fig. 11. Evolution of N_{pG} against Fr_G.

significantly modify the state of homogeneity induced by the mixing process. Additional pouring effect due to the emptying is consequently not the major operation causing particle transport.

Our major aim in this paper was to illustrate that u_{ch} is a key process parameter and consequently should be considered to analyse homogenization data with a planetary mixer. Analysis of

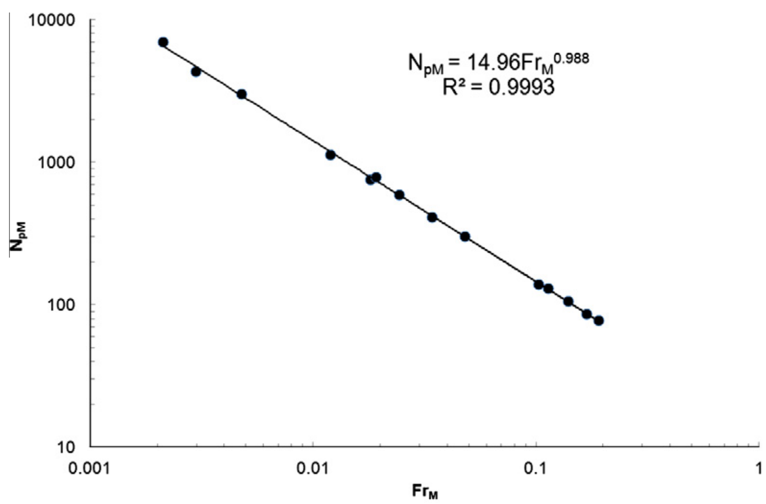

Fig. 12. Evolution of N_{pM} against Fr_G.

power consumption measurements, made before emptying, confirmed the predominant influence of this factor.

Fig. 11 shows the evolution of N_{pG} against Fr_G. Each symbol represents a different speed ratio. This figure proves that the speed ratio and the Froude number have a strong influence on the power consumption of the mixer. For a fixed value of the speed ratio, the exponent of the power law is equal to -1. This value is in agreement with the result obtained by Knight et al. [11].

Fig. 12 shows that all power consumption data can be gathered on a unique curve when u_{ch} is introduced.

This result ascertains, for another target variable, that u_{ch} governs the flow of powders. It can be noted that data for power consumption are less scattered than those obtained for the mixing time. This was expected since power measurements are more accurate than mixing time data (no disturbing effect of discharge procedure and associated evaluation).

5. Conclusions

This work provides guidelines to obtain a concise set of dimensionless numbers governing power and mixing time for a planetary mixer homogenizing granular media. Modified Froude, power and mixing time numbers for a planetary mixer were developed in the case of the mixing of free-flowing granular materials. These modified dimensionless numbers proposed are a generalization of the well-known mixing and power numbers used to describe a conventional mixer.

This study tends to prove (i) the powerful application field of dimensional analysis, (ii) that boundaries should not be considered between granular (free flowing powder) and fluid media, even if, of course, viscosity cannot be considered in the granular medium.

Indeed, it illustrates here that u_{ch} governs also transport phenomena involving granular media as obtained with other mixing processes involving gas/liquid [23] and miscible viscous liquids [22–23] with planetary mixers.

In future work, we will study mixtures consisting of cohesive powders, for which inter-particle forces are dominating particle motion. It is expected that such systems may exhibit different behavior while operated in such a mixer.

References

[1] N. Harnby, M.F. Edwards, A.W. Nienow (Eds.), Mixing in the Process Industries, Buttetworths, London, 1985. p. 42–61.
[2] M. Poux, P. Fayolle, J. Bertrand, D. Bridoux, J. Bousquet, Powder mixing: some practical rules applied to agitated systems, Powder Technol. 68 (1991) 213–234.
[3] J. Bridgwater, Mixing of particles and powders: where next?, Particuology 8 (2010) 563–567
[4] G. Boehm, Report on the industry blend uniformity practices survey, Pharm. Technol. August (2001) 20–26.
[5] A. Rosato, K.J. Strandburg, F. Prinz, R.H. Swendsen, Why the Brazil nuts are on top: size segregation of particulate matter by shaking, Phys. Rev. Lett. 58 (1987) 1038–1051.
[6] J.M. Ottino, D.V. Khakhar, Fundamental research in heaping, mixing and segregation of granular materials: challenges and perspectives, Powder Technol. 121 (2001) 117–122.
[7] J.C. Williams, The segregation of particulate materials – a review, Powder Technol. 15 (1976) 245–251.
[8] S. Massol-Chaudeur, H. Berthiaux, J.A. Dodds, The development of a static segregation test to evaluate the robustness of various types of powder mixtures, Trans. IChemE, Part C – Food Bioprod. Process. 81 (2003) 106–118.
[9] L.T. Fan, Y.M. Chen, F.S. Lai, Recent developments in solids mixing, Powder Technol. 61 (3) (1990) 255–287.
[10] Y.L. Ding, R.N. Forster, J.P.K. Seville, D.J. Parker, Scaling relationships for rotating drums, Chem. Eng. Sci. 56 (2001) 3737–3750.
[11] P.C. Knight, J.P.K. Seville, A.B. Wellm, T. Instone, Prediction of impeller torque in high shear powder mixers, Chem. Eng. Sci. 56 (2001) 4457–4471.
[12] K. Miyanami, Mixing, in: K. Linoya, K. Gotoh, K. Higashitani (Eds.), Powder Technology Handbook, Marcel Dekker, New York, 1991, pp. 595–612.
[13] M. Sato, Y. Abe, K. Ishii, T. Yano, Power requirement of horizontal ribbon mixers, J. Soc. Powder. Technol. Jpn. 14 (1977) 441–447.
[14] M. Sato, K. Miyanami, T. Yano, Power requirement of horizontal cylindrical mixer, J. Soc. Powder. Technol. Jpn. 16 (1979) 3–7.
[15] W. Entrop, in: Proc. European Conference On Mixing in the Chemical and Allied Industries, vol. D1, Mons, Belgium, 1978, pp. 1–14.
[16] P.A. Tanguy, F. Bertrand, R. Labrie, E. Brito De La Fuente, Numerical modelling of the mixing of viscoplastic slurries in a twin blade planetary mixer, Trans. IChemE 74 (Part A) (1996) 499–504.
[17] P.A. Tanguy, F. Thibault, C. Dubois, A. Aït-Kadi, Mixing Hydrodynamics in a double planetary mixer, Trans. IChemE 77 (Part A) (1999) 318–323.
[18] M. Landin, P. York, M.J. Cliff, R.C. Rowe, Scaleup of a pharmaceutical granulation in planetary mixers, Pharm. Develop. Technol. 4 (1999) 145–150.
[19] G. Zhou, P.A. Tanguy, C. Dubois, Power consumption in a double planetary mixer with non-Newtonian and viscoelastic material, Trans. IChemE 78 (Part A) (2000) 445–453.
[20] T. Jongen, Characterization of batch mixers using numerical flow simulations, AIChE J. 46 (2000) 2140–2150.
[21] G. Delaplace, L. Bouvier, A. Moreau, R. Guérin, J.C. Leuliet, Determination of mixing time by colourimetric diagnosis-application to a new mixing system, Exp. Fluids 36 (2004) 437–443.
[22] G. Delaplace, R. Guérin, J.C. Leuliet, Dimensionnal analysis for planetary mixer: modified power and Reynolds numbers, AIChE J. 51 (2005) 3094–3100.
[23] G. Delaplace, R.K. Thakur, L. Bouvier, C. André, C. Torrez, Dimensional analysis for planetary mixer: mixing time and Reynolds numbers, Chem. Eng. Sci. 62 (2007) 1442–1447.
[24] G. Delaplace, P. Coppenolle, J. Cheio, F. Ducept, Influence of whip speed ratios on the inclusion of air into a bakery foam produced with a planetary mixer device, J. Food Eng. 108 (2012) 532–540.
[25] J.F. Demeyre, Caractérisation de l'homogénéité de mélange de poudres et de l'agitation en mélangeur Triaxe, PhD Thesis Report, Institut National Polytechnique de Toulouse, France, 2007.
[26] M. Zlokarnik, Stirring: Theory and Practice, WILEY-VCH verlag GmbH, Weinheim, Germany, 2001.
[27] H. Hausner, Friction conditions in a mass of metal powder, Int J Powder Metall 3 (1967) 7–13.
[28] R.L. Carr, Evaluating flow properties of solids, Chem. Eng. 18 (1965) 163–168.
[29] B. Daumann, H. Nirschl, Assessment of the mixing efficiency of solid mixtures by means of image analysis, Powder Technol. 182 (2008) 415–423.
[30] A. Realpe, C. Velázquez, Image processing and analysis for determination of concentrations of powder mixtures, Powder Technol. 134 (2003) 193–200.
[31] B. Daumann, A. Fath, H. Anlauf, H. Nirschl, Determination of the mixing time in a discontinuous powder mixer by using image analysis, Chem. Eng. Sci. 64 (2009) 2320–2331.
[32] P.M.C. Lacey, Developments in the theory of particle mixing, J. Appl. Chem. 4 (1954) 257–268.
[33] L.T. Fang, R.H. Wang, On mixing indices, Powder Technol. 11 (1975) 27–32.
[34] H. Berthiaux, Mélange et homogénéisation des solides divisés, in: Techniques de l'ingénieur, Traité Génie des Procédés, J 3397, 2002, pp. 1-20.